



Paper Type: Original Article

## Multiple Inspection: A Novel Ultrasonic Phased Array Technique for Simultaneous Surface and Internal Defect Evaluation

Elham Bashiri<sup>1,\*</sup> , Atefeh Ashoori<sup>1</sup> 

<sup>1</sup>Department of Technical Inspection Engineering, Petroleum University of Technology, Abadan, Iran; elham.bashiri73@gmail.com; ati.ashoori1372@gmail.com.

### Citation:

Received: 05 December 2024

Revised: 16 March 2025

Accepted: 20 June 2025

Bashiri, E., & Ashoori, A. (2025). Multiple inspection: A novel ultrasonic phased array technique for simultaneous surface and internal defect evaluation. *International journal of researches on civil engineering with artificial intelligence*, 2(3), 117-126.


### Abstract


Reducing inspection time while improving defect detection reliability has become a major challenge in modern industrial applications. Recent advances in ultrasonic technologies have enabled more efficient and accurate Nondestructive Evaluation (NDE) of critical components. Among these technologies, Phased Array Ultrasonic Testing (PAUT) systems offer exceptional flexibility in beam steering and wavefront control, significantly enhancing inspection capabilities. In this study, a Finite Element (FE) simulation is presented to investigate a novel ultrasonic inspection approach termed Multiple Inspection. The proposed technique combines the beam-steering capability of phased array ultrasonics with efficient Rayleigh wave generation to simultaneously inspect both the near-surface region and the internal volume of a component within a single examination. By integrating the advantages of bulk-wave and surface-wave inspections, the method provides comprehensive information regarding different defect types while reducing overall inspection time. Simulation results demonstrate the capability of the proposed approach to detect internal cracks and surface defects concurrently with high reliability. The findings suggest that multiple inspections can improve inspection efficiency and provide a promising alternative to conventional ultrasonic testing procedures for industrial NDE.

**Keywords:** Nondestructive evaluation, Phased array ultrasonic testing, Finite element simulation, Rayleigh waves, Surface defects, Internal cracks.

## 1 | Introduction

The simultaneous detection of internal and surface defects using a single ultrasonic inspection procedure represents an important objective in Nondestructive Evaluation (NDE). Conventional ultrasonic techniques

 Corresponding Author: elham.bashiri73@gmail.com

 <https://doi.org/10.48314/ijrceai.v2i3.49>



Licensee System Analytics. This article is an open-access article distributed under the terms and conditions of the Creative Commons Attribution (CC BY) license (<http://creativecommons.org/licenses/by/4.0>).

are generally optimized either for volumetric flaw detection or for surface defect characterization, often requiring multiple inspections to obtain complete information about the structural integrity of a component. Such approaches inevitably increase inspection time, operational costs, and procedural complexity.

Several studies have attempted to overcome these limitations by developing methods capable of evaluating different types of defects within a unified framework [1], [2]. However, to the best of the authors' knowledge, no previous work has investigated a phased-array-based technique capable of simultaneously detecting both surface discontinuities and internal cracks through a single inspection process. The present study introduces a novel concept referred to as Multiple Inspection, which addresses this challenge through Finite Element (FE) modeling and simulation.

Numerical simulation has become an indispensable tool in ultrasonic testing research because it provides valuable insight into wave propagation phenomena and enables optimization of inspection parameters before experimental implementation. FE modeling, in particular, facilitates the mathematical representation of complex physical systems and predicts their responses under varying input conditions. Early applications of FE methods in ultrasonic modeling were reported by Ludwig and Lord [3], establishing the foundation for subsequent developments in ultrasonic simulation [4]. More recently, FE simulations of Phased Array Ultrasonic Testing (PAUT) have played a significant role in improving transducer performance, optimizing beam configurations, and identifying favorable inspection conditions [5].

Among the advanced ultrasonic techniques, Time-of-Flight Diffraction (ToFD) has attracted considerable attention because of its high accuracy in detecting and sizing internal planar defects. Unlike conventional pulse-echo methods, ToFD relies on measuring the travel time of waves diffracted from crack tips rather than signal amplitude. This time-based approach enables highly accurate determination of flaw dimensions, particularly defect depth and length. FE investigations of ToFD have been reported by Baskaran et al. [6] and Honarvar and Khorasani [7].

In contrast, Rayleigh waves are particularly suitable for the detection and characterization of surface-breaking defects. These waves propagate along free surfaces while their amplitude decays exponentially with depth. Because their energy is concentrated near the surface, Rayleigh waves exhibit high sensitivity to shallow discontinuities and small surface flaws. Furthermore, their ability to follow complex geometries enables inspection of regions that may be inaccessible to other ultrasonic wave modes.

Previous studies have demonstrated the effectiveness of Rayleigh-wave-based inspection techniques. Date et al. [8] reported highly accurate characterization of slots with depths as small as 0.8 mm, achieving a standard deviation below 0.1 mm. Hévin et al. [9] estimated the depth of surface cracks in concrete with an accuracy of approximately 15% using spectral analysis of transmitted waves. Similarly, Scala and Bowles [10] measured slots as shallow as 0.5 mm with an accuracy better than 50  $\mu\text{m}$  through transmitted near-field measurements.

Building upon these developments, this work proposes a novel Multiple Inspection technique that exploits the beam steering capability of phased array ultrasonics to generate both bulk waves and Rayleigh waves within a single inspection sequence. Through FE simulation, the proposed method is evaluated for its ability to simultaneously identify internal cracks and surface defects. The results demonstrate the feasibility of achieving comprehensive defect assessment with reduced inspection time, thereby enhancing the efficiency of industrial NDE.

## 2 | Finite Element Method Modelling of Time-of-Flight Diffraction Method

The commercial Finite Element Method (FEM) package ABAQUS6.11 is used for two-dimensional modelling of ultrasonic wave propagation. The physical properties of the block are as follows:  $E = 60$  GPa,  $\rho = 2240$  kg/m<sup>3</sup>, and  $\nu = 0.244$ . The entire area of the sample is discretised into a standard two-dimensional spatial square plane strain elements (CPE4R) with linear shape functions and four nodes, where each node has two degrees of freedom with respect to displacement. In order to get more accurate results, we can

decrease the element size, but there are limitations. These limitations occurred due to the limited computer system capacity to calculate an enormous calculation needed for simulation. By the previous work [4], mesh size ( $\Delta d$ ) should satisfies to *Eq. (1)*:

$$\Delta d \leq \lambda/15, \quad (1)$$

Where  $\lambda_{\min}$  is the shortest wavelength at the excitation frequency of the simulated waves and  $\Delta d$  is the dimension of the element. Our trial and error studies showed that in order to have a low computation time and good convergence, a mesh size in the order of  $5 \times 10^{-5}$  m should be chosen.

## 2.1 | Modeling of Transmitting Transducer

In this study actual piezoelectric mechanisms has been modeled by the relevant transient pressure excitation. This excitation is a narrowband tone burst pulse of a certain frequency which is applied on the 0.3 mm distance on a top surface of sample block. 32 elements designed and excited, In other words Ultrasonic pulse was introduced as a transient excitation pulse which applied as pressure on width of each element. This pulse is given in *Eq. (2)* where  $f$  is the excitation frequency and  $N$  is the number of cycles force.

$$F = \left[ 1 - \cos\left(\frac{2\pi f}{N}t\right) \right] \cos(2\pi f t), \quad 0 < t < \frac{N}{f}. \quad (2)$$

In order to propagate an oblique ultrasonic wave by phased array probe, we use a time delay law. These time delays which applied on adjacent phased array element computed with Huygens's principle that stated in *Eq. 3*:

$$\Delta t = \frac{d \sin \theta_s}{C}, \quad (3)$$

where "d" is distance between two adjacent elements,  $\theta_s$  is steering angle or propagation angle, "C" is longitudinal wave velocity in the media and  $\Delta t$  is time delay between two adjacent elements.

## 2.2 | Modeling of Receiving Transducer

Since the basic of piezoelectric transducer operation is the conversion of electrical pulses to mechanical pressure and inverse, therefore we consider a "set point" on surface as receiver probe. Acceleration amplitude variations of this "set point" regarded as amplitudes variations in simulations in order to increase accuracy and quality of simulations.

## 3 | Convergence Test

One of the most important part of validation of simulated model is "convergence test" for FEM simulation. In order to discuss about convergence results, different size of element is considered. Amplitude diagram of center node of probe from top crack tip is used to discuss about converging results. Signal to noise ratio is obtained from received signals and plotted against element size in *Fig. 1*. For elements which are smaller than  $50 \mu\text{m}$  size, SN ratio is stabilized and has a constant value approximately.

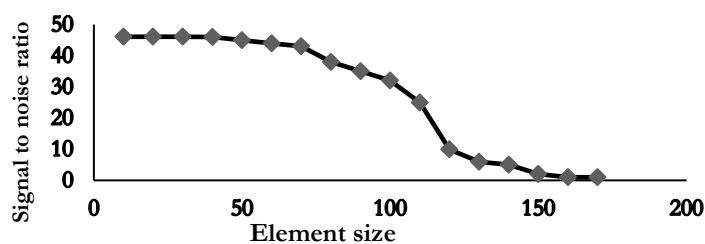


Fig. 1. Signal to noise ratio obtained from received signals.

## 4 | Interaction of Phased Array Ultrasonic Waves with Embedded Crack

After a phased array transducer is excited, longitudinal (I) and shear (II) waves are propagated in bulk of simulated steel block. Also lateral longitudinal wave (III), lateral shear wave (IV) and Rayleigh wave (V) are transmitted along the surface. Head wave is denoted by (VI) (Fig. 2). After the Longitudinal wave incident to crack, sharp crack tip, like a source of wave, starting out a wave emission. These diffracted waves from crack tips applied for ToFD method, the first diffracted wave from top crack tip which denoted by “VII” is “Top Longitudinal Diffraction” wave or “TLD”. Second diffracted wave is “Top shear diffraction” wave or “TSD”, indicated by “VIII”, also bottom diffraction waves denoted by (IX) and (X) as shown in Figs. 3 and 4.

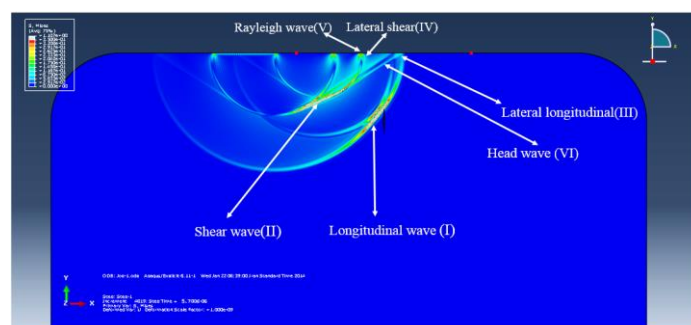


Fig. 2. Snapshot of Abaqus viewport at 5.7( $\mu$ s).

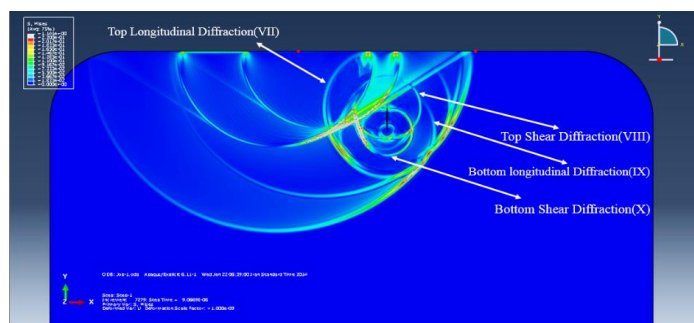


Fig. 3. Snapshot of Abaqus viewport at 9.066( $\mu$ s).

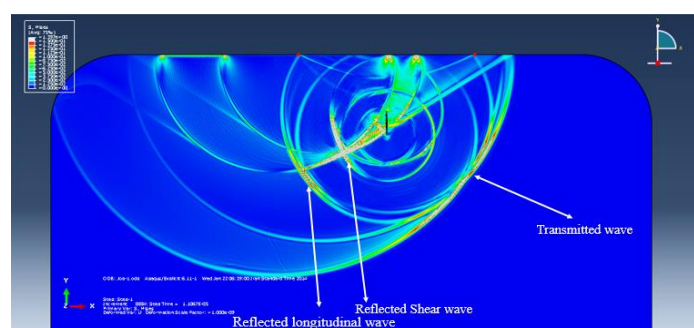


Fig. 4. Snapshot of Abaqus viewport at 11.088( $\mu$ s).

## 5 | Effect of Wave Angle Variation on Amplitude of Waves

Fig. 6 is the diagram of variation of “Lateral longitudinal” wave amplitude by change in angle of wave. Slope of the curve is greater for angles which are wider than 60' in other words “Lateral longitudinal” wave amplitude increased more. For angles less than 40' “Lateral longitudinal” received amplitudes reduced too much in comparison with angles greater than 60'. Fig. 6 indicates that “Lateral longitudinal” amplitudes is related to angle of wave significantly and if it is used for surface defect detection, then wave angle should be considered as a high limitative parameter. “Lateral shear” wave amplitude variations plotted against angle wave variations. Measured amplitudes increases by increasing the angle of oblique wave. Fig. 7 denotes the high dependency of “Lateral shear” wave on wave angles. For angles which less than 45' “Lateral Shear” wave measured amplitude has small amount and it is hard to distinguish it from noises. Fig. 8 indicates the variation of Rayleigh wave amplitudes by change in angle of wave. It is obvious from this figure that Rayleigh wave amplitudes aren't affected by angle variation of wave. According to Figs. 6 and 7 which show the effects of change in wave angle parameter on received signals, it can be concluded that a single type of surface waves which is not affected by angle variations is Rayleigh wave. Rayleigh wave is not impressed considerably with angle variation and it has constant amplitudes value even for oblique waves which are smaller than 40 degree.

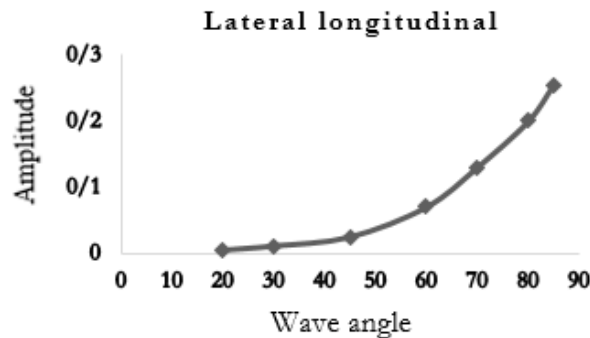


Fig. 6. Effect of angle variation on amplitude of lateral longitudinal wave.

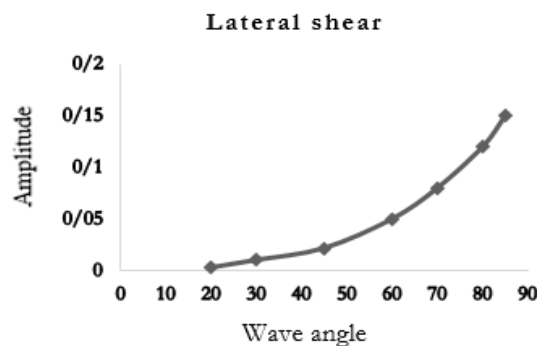


Fig. 7. Effect of angle variation on amplitude of lateral shear wave.

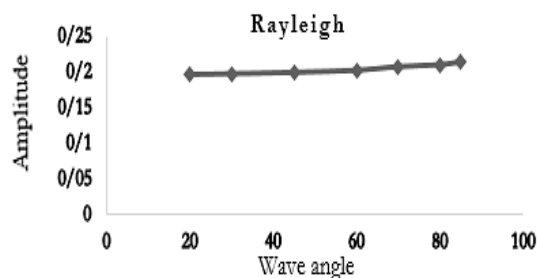


Fig. 8. Effect of angle variation on amplitude of Rayleigh wave.

## 6 | Effect of Distance on Amplitude of Surface Waves

As shown in *Fig. 9*, the lateral longitudinal wave amplitude decreases by increasing the distance of receiving transducer from transmitter. Received “Lateral longitudinal” echo for a transducer which is located at 1cm distance from the transmitting transducer has maximum value due to short distance between transmitter and receiver. In the first 4cm distance from transmitter, “Lateral longitudinal” wave amplitude decreases rapidly, but in the next 4cm distance, the slope of curve is much less. *Fig. 9* demonstrates that lateral longitudinal wave has high decreasing value specially at near distances from transmitting probe and when the “Lateral longitudinal” wave travels 8cm, its amplitude reduced significantly. “Lateral shear” variations with distance is plotted in *Fig. 10*. After 4cm distance “Lateral shear” wave decreases significantly, between 2cm and 4cm slope of curve i.e. ratio of “Lateral shear” amplitude variations with respect to distance from transmitter transducer is greater than other parts of the curve, in other word at this area “Lateral shear” wave amplitude reduced a lot. “Lateral shear” and “Lateral longitudinal” wave amplitude decrease a lot after passing 6cm and 8cm respectively. It is a warning notation in surface defect detection. If defects locate out of this zone (6cm and 8cm from transmitting transducer), using “Lateral longitudinal” and “Lateral shear” waves for defect detection have not recognizable results. *Fig. 11* shows the relation between Rayleigh wave amplitude and Rayleigh wave travelling distance. Rayleigh waves aren’t affected by distance variations. It has constant amplitudes even in far distances which other types of surface waves disappear. In addition to positive feature which stated at previous section, Constant amplitude of Rayleigh wave with distance variations is another main positive aspect of Rayleigh waves for surface defect detection.

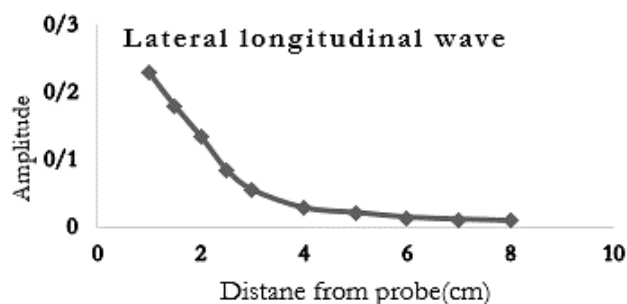


Fig. 9. Effect of variation of distance on amplitude of lateral longitudinal waves.

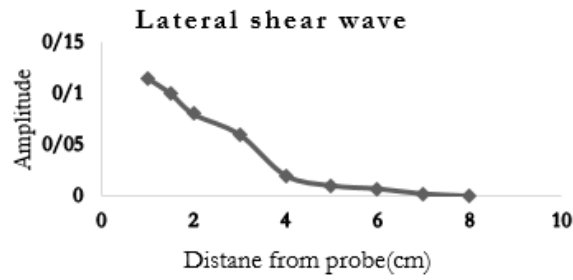


Fig. 10. Effect of variation of distance on amplitude of lateral longitudinal waves.

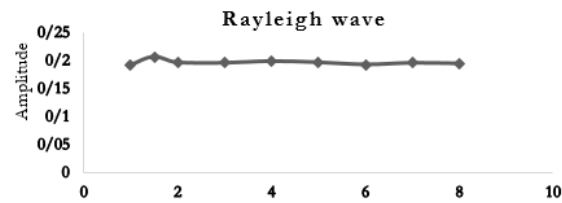


Fig. 11. Effect of variation of distance on amplitude of lateral longitudinal waves.

## 7 | Crack Sizing by Time-of-Flight Diffraction with Single Probe Technique in Various Depths

Fig. 12 shows his method schematically. Crack depth varies from 10mm to 75mm. Crack length is 7mm and is perpendicular to scanning surface. Normal distance between centerline of probe and crack body(S) is 2.5cm. cracks were located in 1,2,3,4,5,5.5,6,6.5,7,7.5 far from surface and normal distance between cracks and centerline of probe is 2.5cm. Diffracted waves from crack tips were detected well and the A-scan was analyzed, results are show in Fig. 13. A-scan signals a sample block with embedded crack in depths 2 shown in Fig. 14. all received echoes before 4( $\mu$ s) which spreads on time axis are initial pulses(V) and appear due to phased array excitation pulses on center node of probe. In Fig. 14 the Top longitudinal diffraction (I) and the Bottom longitudinal diffraction (II) are received at 11.088( $\mu$ s) and 12.680( $\mu$ s) and define a crack size with 3.9% error. Shear diffraction signals are sensed after longitudinal diffraction waves.

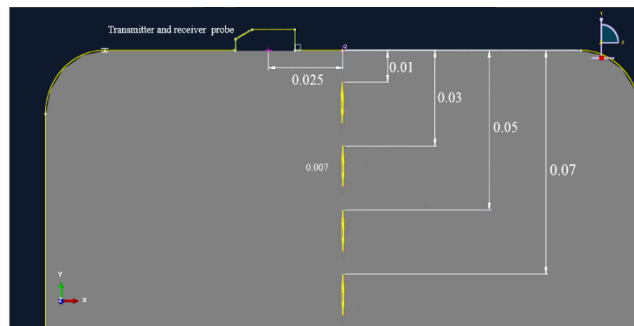


Fig. 12. Crack sizing by ToFD with single probe technique in various depths.

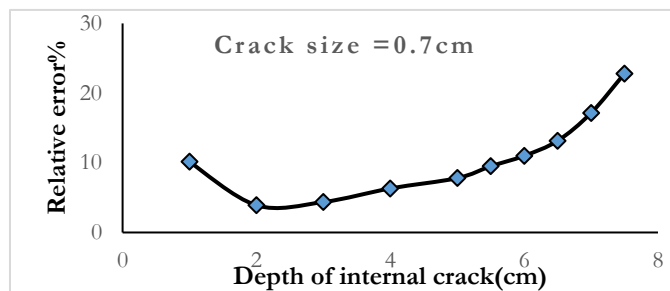


Fig. 13. the variation of relative error for crack sizing by ToFD method with single probe in different depths.

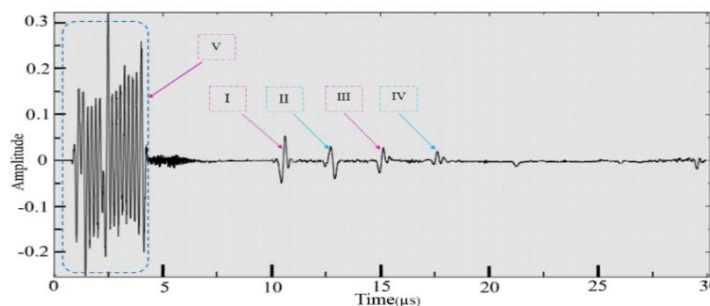
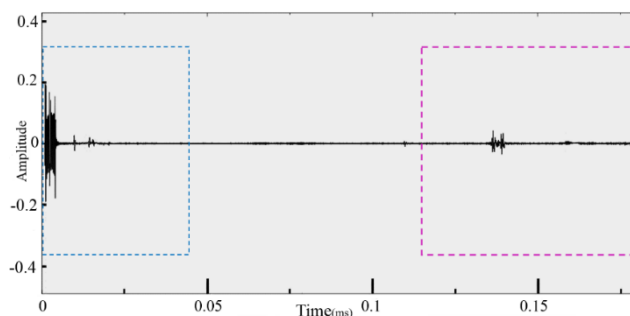


Fig. 14. A-scan signal from sample which has a crack at 2cm depth.

## 8 | Multiple Detection of Surface and Planar Defect

Effect of angle variation and also increasing distance on surface waves has been discussed in the section of Rayleigh wave, from two main aspects Rayleigh wave is in priority for surface defect detection. At first Rayleigh wave constant amplitude by increasing distance motivate us to applying this wave for defect detection, another aspect is amplitude stability by angle variations. ToFD with single probe simulated completely. In this section, single probe is used as the both transmitter and receiver probe for NDE of crack and surface defect detection simultaneously for the first time. A-scan received signal clearly shows the crack diffraction echoes and also Rayleigh reflection waves. Finally an A-scan which determine defects and also characterize internal crack is obtained. Fig. 15.a shows A-scan of sample which has a crack of 1cm length in 2cm depth and also surface defect in 22.14cm far from the center of phased array transducer. Fig. 15.b and Fig. 15.c is magnifying view of first 40(μs) and last 40(μs), reflected and diffracted waves can be observed in Fig. 15.a, because of long A-scan time, parts of it, is enlarged. In first 40(μs), embedded crack is detected by ToFD method and evaluation of diffraction received echoes indicates a crack of 9.5mm length which has 4.2% error.



a.

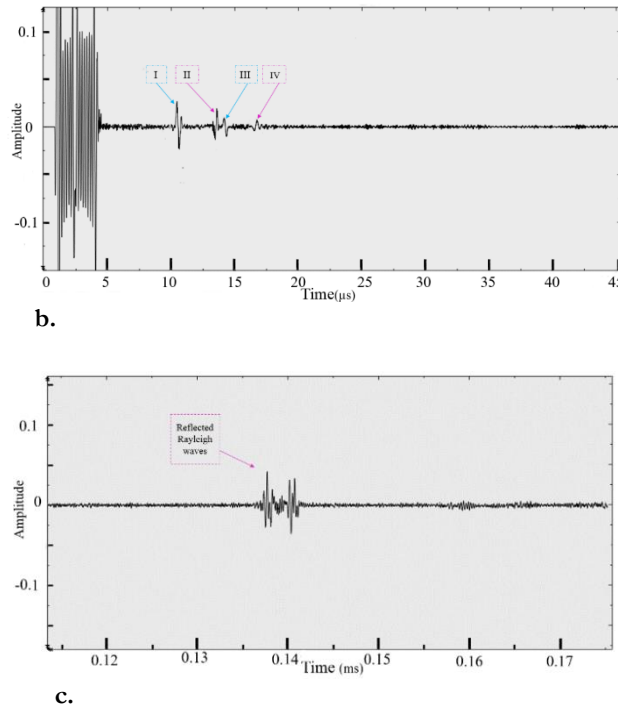


Fig. 15. a. multiple A-scan signal which shows both internal crack and surface defect, b. magnified view of first 40(μs) of Fig. 15.a which shows a 9.57mm crack inside a block, and c. magnified view of last 40(μs) of Fig. 15.a which shows a surface defect at 19.967cm far from probe.

Accuracy of Rayleigh wave in surface defect detection shown on Fig. 16. The error growth rate variation is minus and low and also after defect distance from probe is increased to 18cm, it descend more.

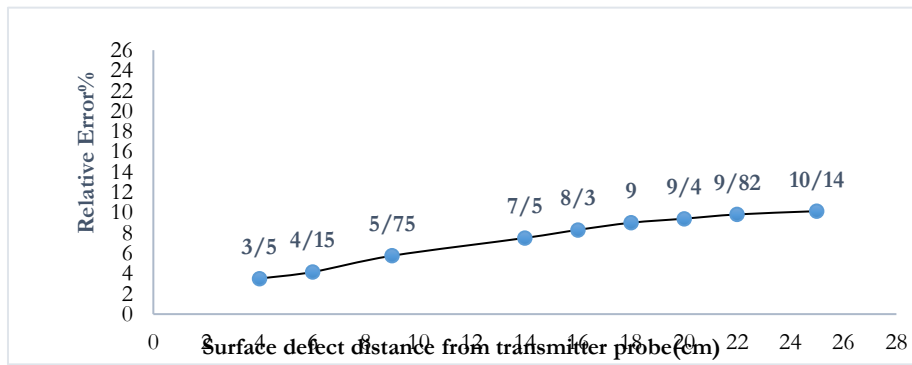


Fig. 16. Accuracy of Rayleigh wave in surface defect detection by increasing defect distance.

## 9 | Conclusion

Between surface waves, Constant amplitude indicates the Rayleigh wave stability on surface. It keeps energy even in far distances which other types of surface waves disappear. Also a single form of surface waves which is not affected by angle variations is Rayleigh wave.

Error variations of ToFD by single probe for crack with constant length in different depths investigated. From depth 1 to 6 cm, a good approximation of crack size obtained. The critical depth range for crack size evaluation is 6 to 8cm in this method.

Simulation of Multiple defect detection, a novel method in defect detection and evaluation which determines an internal crack and surface defect simultaneously has been done, this method based on high capabilities of ultrasonic phased array system.

Accuracy of Rayleigh wave in surface defect detection determined and surface defect detected in 24cm distance by less than 10%.

## References

- [1] Ernst, R., Weder, M., & Dual, J. (2012). Multiple defect detection by applying the time reversal principle on dispersive waves in beams. *18th world conference on nondestructive testing* (pp. 540-548). South African Institute for Non-Destructive Testing (SAINT), Durban, South Africa.  
<https://www.proceedings.com/content/017/017743webtoc.pdf>
- [2] Zhang, J., Drinkwater, B. W., Wilcox, P. D., & Hunter, A. J. (2010). Defect detection using ultrasonic arrays: The multi-mode total focusing method. *NDT & e international*, 43(2), 123–133.  
<https://doi.org/10.1016/j.ndteint.2009.10.001>
- [3] Ludwig, R., & Lord, W. (1986). Developments in the finite element modeling of ultrasonic NDT phenomena. In *Review of progress in quantitative nondestructive evaluation* (pp. 73-81). Plenum Press.  
<https://doi.org/10.1007/978-1-4613-1893-4>
- [4] Connolly, G. D. (2009). *Modelling of the propagation of ultrasound through austenitic steel welds* [Thesis].
- [5] Abdollahi-Mamoudan, F., Ibarra-Castanedo, C., & Maldague, X. P. V. (2025). Non-destructive testing and evaluation of hybrid and advanced structures: A comprehensive review of methods, applications, and emerging trends. *Sensors*, 25(12), 1–42. <https://doi.org/10.3390/s25123635>
- [6] Baskaran, G., Rao, C. L., & Balasubramaniam, K. (2007). Simulation of the ToFD technique using the finite element method. *Insight-non-destructive testing and condition monitoring*, 49(11), 641–646.  
<https://doi.org/10.1784/insi.2007.49.11.641>
- [7] Honarvar, F., & Khorasani, S. (2010). *Simulation of time of flight diffraction (ToFD) technique by finite element method*. Online Workshop, NDT.net – The e-Journal of Nondestructive Testing.  
[https://www.ndt.net/article/SimNDT2010/papers/16\\_Honarvar\\_Rev1.pdf](https://www.ndt.net/article/SimNDT2010/papers/16_Honarvar_Rev1.pdf)
- [8] Date, K., Shimada, H., & Ikenaga, N. (1982). Crack height measurement — An evaluation of the accuracy of ultrasonic timing methods. *NDT international*, 15(6), 315–319. [https://doi.org/10.1016/0308-9126\(82\)90068-2](https://doi.org/10.1016/0308-9126(82)90068-2)
- [9] Hévin, G., Abraham, O., Pedersen, H. A., & Campillo, M. (1998). Characterization of surface cracks with Rayleigh waves: A numerical model. *NDT & e international*, 31(4), 289–297. [https://doi.org/10.1016/S0963-8695\(98\)80013-3](https://doi.org/10.1016/S0963-8695(98)80013-3)
- [10] Scala, C. M., & Bowles, S. J. (2000). Laser ultrasonics for surface-crack depth measurement using transmitted near-field rayleigh waves. *AIP conference proceedings* (pp. 327–334). AIP Publishing.  
<https://doi.org/10.1063/1.1306068>